Radiation induced defects in $Sr_2B_5O_9Br:Ce^{3+}$ storage phosphor

2004 J. Phys.: Condens. Matter 16 4131

(http://iopscience.iop.org/0953-8984/16/23/027)

INSTITUTE OF PHYSICS PUBLISHING JOURNAL OF PHYSICS: CONDENSED MATTER

J. Phys.: Condens. Matter **16** (2004) 4131–4138 PII: S0953-8984(04)75895-6

Radiation induced defects in $Sr_2B_5O_9Br:Ce^{3+}$ storage phosphor

A V Sidorenko[1,5], A J J Bos[1], P Dorenbos[1], C W E van Eijk[1], P A Rodnyi[2], I V Berezovskaya[3], V P Dotsenko[3], O Guillot-Noel[4] and D Gourier[4]

[1] Interfaculty Reactor Institute, Delft University of Technology, Mekelweg 15, 2629 JB Delft, The Netherlands
[2] St Petersburg State Technical University, Polytekhnicheskaya 29, 195251 St Petersburg, Russian Federation
[3] A V Bogatsky Physico-Chemical Institute, Ukranian Academy of Science, 65080 Odessa, Ukraine
[4] Laboratoire de Chimie Appliquée de l'Etat Solide, UMR 7574, ENSCP, 11 rue Pierre et Marie Curie, 75231 Paris Cedex 05, France

E-mail: asidore@iri.tudelft.nl

Received 29 January 2004, in final form 31 March 2004
Published 28 May 2004
Online at stacks.iop.org/JPhysCM/16/4131
DOI: 10.1088/0953-8984/16/23/027

Abstract

Radiation induced defects in polycrystalline pure and Ce^{3+} doped $Sr_2B_5O_9Br$ storage phosphors have been investigated using EPR and optical absorption methods. The EPR of irradiated pure $Sr_2B_5O_9Br$ represents two overlapping spectra in the 335–340 mT range from paramagnetic electron and hole trapping centres, which are stable at room temperature. These centres are attributed to $F(Br^-)$ and O^-_{Br} centres, i.e. an electron trapped in a bromine vacancy and a hole trapped on an oxygen ion at a bromine site. The $1s \rightarrow 2p$ transitions of $F(Br^-)$ centres cause the optical absorption band at 560 nm. Another observed absorption band at 365 nm was attributed to the transitions of O^- centres. Thus electron and hole trapping in pure $Sr_2B_5O_9Br$ occurs in V_{Br} and O^{2-}_{Br} aggregates, which are created during the synthesis.

EPR and optical absorption measurements on Ce^{3+} doped $Sr_2B_5O_9Br$ reveal similar defects as in pure material. It is very likely that the same defects take part in the processes of thermally and photo-stimulated luminescence.

1. Introduction

There is a growing interest in the development of low γ-ray sensitive storage phosphor materials for use in position sensitive thermal neutron detection. Haloborates represent promising

[5] Author to whom any correspondence should be addressed.

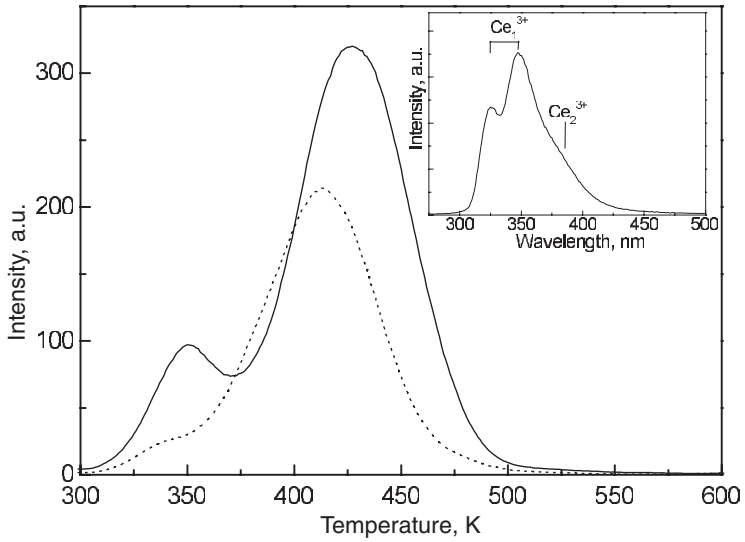

Figure 1. The TL glow curves of $Sr_2B_5O_9Br$:1% Ce^{3+} (solid curve) and $Sr_2B_5O_9Cl$:0.5% Ce^{3+} (dotted curve) recorded with 1 K s^{-1} heating rate after β-irradiation. In the inset the x-ray excited emission spectrum of $Sr_2B_5O_9Br$:1% Ce^{3+} is shown and the bands attributed to two types of Ce^{3+} centre are indicated.

materials for such applications [1, 2]. The aim of this study is to reveal the nature of trapping defects, which are involved in the storage process in haloborates.

The current understanding of the nature of electron and hole trapped centres in the most promising storage phosphors was set out in [3]. There are several types of photostimulable x-ray storage phosphor known among alkaline and alkaline-earth halides, and BaFBr doped with Eu^{2+} is the most successful x-ray storage phosphor used for digital radiography so far. In all known alkaline-halide storage phosphors x-ray irradiation generates F centres as photostimulable electron trapping centres. The nature of photostimulable hole trapping defects is less understood and it is generally connected to impurity ions.

The luminescence and thermally stimulated luminescence (TL) properties of $Sr_2B_5O_9Br$ doped with Ce^{3+} were reported previously in [4]. The general conclusions made are summarized as follows: two types of Ce^{3+} centre are present in $Sr_2B_5O_9Br$:Ce^{3+} and they are associated with isolated Ce_1^{3+} and locally charge compensated Ce_2^{3+} centres. Probably, several charge compensation defects are involved in formation of the Ce_2^{3+} centre. The TL glow curves of $Sr_2B_5O_9Br$:Ce^{3+} consist of two peaks at 350 and 430 K, as shown in figure 1. The TL emission of $Sr_2B_5O_9Br$:Ce^{3+} related to the low temperature peak originates from Ce_1^{3+} centres. The emission in the 430 K peak is from both Ce_1^{3+} and Ce_2^{3+} centres. The high temperature peak is of interest from a practical point of view, because it is stable at room temperature and gives the most intense TL and PSL response. The position of the high temperature TL peak depends on the ligand anion (Cl^- or Br^-), as can be seen in figure 1. It is shifted towards lower temperature in the case of chlorides.

In this paper the results of EPR and optical absorption studies on powder bromborate samples will be presented. The EPR study on a powder sample in principle gives less information than that on a single crystal. However, qualitative information about types of defect, their number and thermal stability can be derived [5]. Optical absorption bands on powder samples were derived from measured diffuse reflectance spectra. As known the positions of diffuse reflection bands and absorption bands coincide [5].

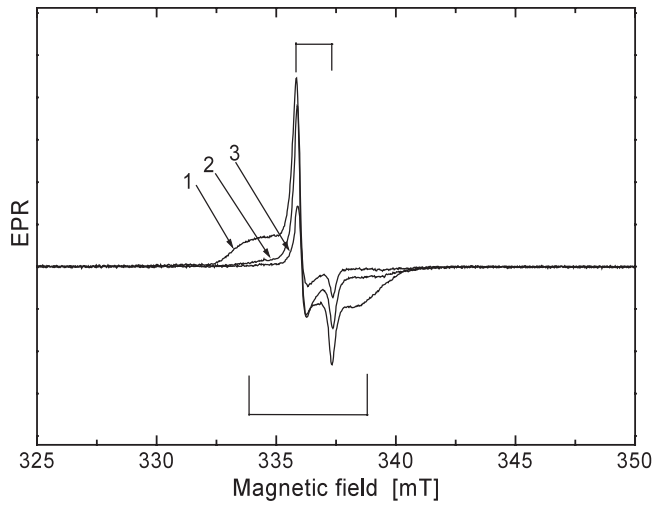

Figure 2. Experimental EPR spectra of x-ray irradiated pure $Sr_2B_5O_9Br$ recorded at 120 K. Each curve was recorded at a different time after irradiation: 10 min (curve 1), 1 day (curve 2) and one week (curve 3) after irradiation. The 'broad' and 'narrow' EPR lines are indicated (see the text). Between experiments the sample was kept in darkness at room temperature.

2. Experimental details

Solid solutions of haloborates were synthesized in the Bogatsky Physico-Chemical Institute using the solid state method as described in [6].

The EPR measurements were carried out at the Laboratory of Applied Chemistry of the Solid State at ENSCP (Paris). A Bruker ESP300e spectrometer was used. The applied microwave frequency was about 9 GHz. All spectra were corrected for the signal of the cavity with an empty sample holder (quartz tube). Irradiation was performed *ex situ* with a Siemens x-ray tube operated at 40 keV and 35 mA. Simulations of EPR powder spectra were carried out using 'WINEPR SimFonia 1.25' software.

Diffuse reflection measurements were performed with a diode array UV/VIS spectrophotometer (HP 8452A) equipped with a 95 mm diameter Spectralon integrating sphere (RSA-HP-84-UV) with an externally mounted xenon light source allowing measurements in the 300–800 nm wavelength range. Large area samples were compared with a calibrated 99% diffuse reflectance standard. Irradiation was performed with a ^{60}Co γ-source with a dose rate 0.7 kGy h^{-1}.

3. Results

3.1. EPR measurements on irradiated pure $Sr_2B_5O_9Br$

Before irradiation no EPR signals in pure $Sr_2B_5O_9Br$ were detected. The EPR spectra of irradiated pure $Sr_2B_5O_9Br$ recorded at 120 K just after irradiation, one day and one week after irradiation are shown in figure 2. The spectrum measured just after irradiation shows the presence of at least two overlapping EPR spectra: one is the broad line with maxima at 334 and 339 mT and another one is the narrow line in the 336–337 mT range. Defects due to the broad EPR line are not stable at room temperature, since this line cannot be observed one day after irradiation, while storing the sample at room temperature. Therefore, it is possible to separate

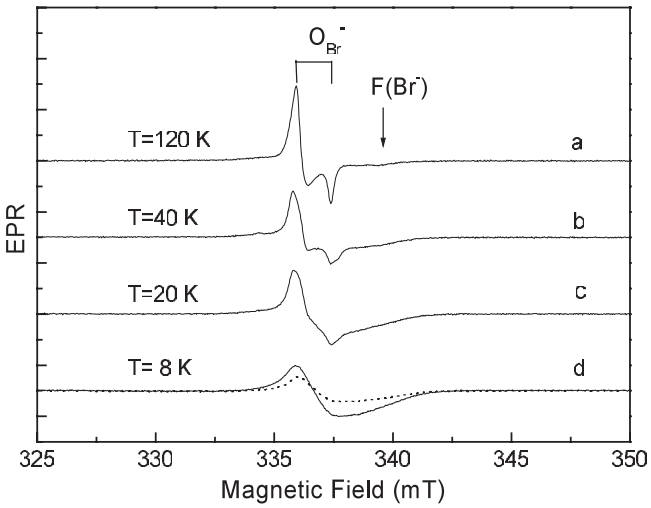

Figure 3. The EPR spectra of x-ray irradiated pure $Sr_2B_5O_9Br$ recorded at different temperatures. Measurements were made one day after irradiation. The EPR spectrum measured at 8 K one week after irradiation is shown as a dotted curve. The attribution of EPR lines to $F(Br^-)$ and O^-_{Br} is explained in the text.

both overlapping signals. From here, the discussion will concern only room temperature stable defects. In figure 3 the evolution with temperature of the EPR spectra recorded one day after irradiation is shown. The shape of the curves changes dramatically with temperature. Moreover, at low temperatures an additional EPR signal at about 340 mT appears. Such a trend in EPR spectra suggests the existence of two types of paramagnetic defect with overlapping EPR spectra in the 336–340 mT range. This point will be discussed further.

3.2. Radiation induced optical absorption spectra of irradiated pure and Ce^{3+} doped $Sr_2B_5O_9Br$

The diffuse reflection spectra of pure and Ce^{3+} doped $Sr_2B_5O_9Br$ were measured. In figures 4 and 5 the differences between the reflection spectra recorded before and after irradiation are plotted. The difference between these spectra represents the radiation induced absorption. The absorption curve of pure $Sr_2B_5O_9Br$ was fitted with two Gaussians with maxima at 365 and 560 nm as shown in figure 4. The broad structures of these peaks must be due to the polycrystalline nature of the sample [5]. It is seen from figure 4 that the relative contribution to the total absorption from these two peaks is the same just after irradiation and two days after irradiation. Therefore, we assume that the two bands originate from trapped hole and electron centres, created under irradiation. Thus, the ratio between the number of electron and hole centres stays constant, but some of them recombine with each other at room temperature, which leads to the decrease in total absorption in figure 4. The nature of these centres will be discussed later.

The treatment of reflection spectra of $Sr_2B_5O_9Br$ doped with Ce^{3+} is more complicated than in the case of pure material. The measurement system is equipped with a diode array for light detection and with a xenon lamp. During the measurements a sample is excited with the whole spectrum of the xenon lamp (270–820 nm). Therefore, in reflection curves the bands due to Ce^{3+} absorption and Ce^{3+} luminescence at 330 and 350 nm are very intense. As can be seen in the inset of figure 5 at a particular wavelength the reflectivity is more than 100%, which

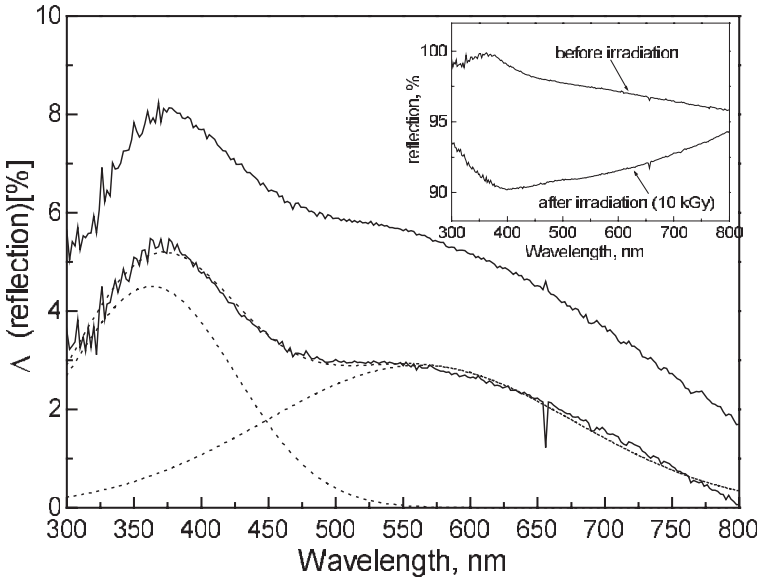

Figure 4. In the inset reflection spectra of pure $Sr_2B_5O_9Br$ recorded before irradiation and after irradiation (10 kGy with ^{60}Co gamma source) are plotted. The difference between them just after irradiation (upper curve) and two days after irradiation (lower curve) is plotted in the main figure. Dotted curves represent a fit of the absorption curve measured two days after irradiation with two Gaussian peaks.

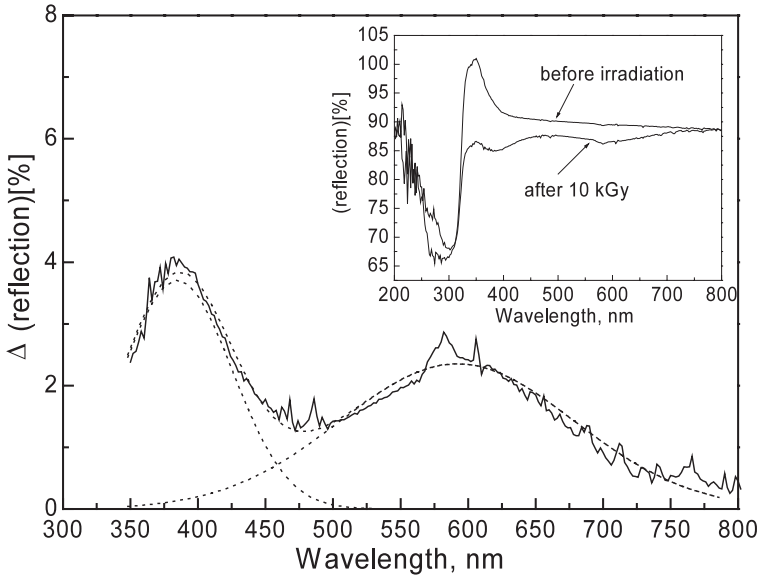

Figure 5. Reflection spectrum of $Sr_2B_5O_9Br$:1% Ce^{3+} recorded prior to irradiation minus the reflection spectrum recorded after irradiation with a ^{60}Co gamma source. The received dose was 10 kGy. Below 350 nm the differential spectrum is not plotted, because of the large error caused by the presence of Ce^{3+} absorption and emission bands. The dotted curves represent a fit of the spectrum with two Gaussian peaks. In the inset reflection spectra of $Sr_2B_5O_9Br$:1% Ce^{3+} recorded before irradiation and after irradiation (10 kGy with a ^{60}Co gamma source) are plotted.

is caused by Ce^{3+} luminescence. In a spectrum obtained just by subtraction of reflection curves before and after irradiation the intense band due to Ce^{3+} luminescence is still present. This can be explained by partial absorption of Ce^{3+} luminescence in the material after irradiation. Therefore, Ce^{3+} emission intensities in reflection curves measured before and after irradiation are different. Because of this an additional subtraction of the Ce^{3+} emission band was done to obtain a correct differential spectrum, and the result is shown in figure 5. This spectrum was fitted with two Gaussians with maxima at 380 and 580 nm.

4. Discussions

4.1. Radiation induced defects in pure $Sr_2B_5O_9Br$

4.1.1. EPR results. The EPR measurements performed at 120 K on irradiated pure $Sr_2B_5O_9Br$ showed the presence of defects which are stable at room temperature and exhibiting the line between 335 and 338 mT (figure 3, curve a). This spectrum can be simulated well by assuming an axial centre with the g-values of $g_\perp = 2.017(0)$ and $g_\parallel = 2.008(5)$. The positive shift of g-values indicates that it is a hole centre. The absence of hyperfine interaction of the spin with boron nuclei (^{11}B has $I = 3/2$ and 18.8% abundance) evidences that the hole is not trapped in the borate network [7].

Based on crystal structure of haloborates two hypotheses about the nature of this defect are proposed. The first one is the creation of a V_k-centre Br_2^- molecule. Usually V_k centres diffuse at temperatures above 120 K, and only some V_{ka} centres, i.e. V_k centres localized close to a defect or impurity, can be stable at room temperature [8]. For the creation of V_k centres a high local symmetry and small distance between halogens is needed [8]. In $Sr_2B_5O_9Br$ the Br–Br distance is 5.9 Å and that is too large for creation of V_k centres.

The absence of hyperfine splitting in figure 3 suggests a centre whose central element has a low abundance of magnetic isotopes. The natural abundance of ^{17}O ($I = 5/2$) is just 0.038%, thus no hyperfine interaction can be observed. There is a high content of oxygen atoms in $Sr_2B_5O_9Br$. Hence, it is reasonable to propose the formation of an oxygen ion in a bromine site (O_{Br}^{2-}) during the synthesis. Such a defect has an additional negative charge and can trap a hole. The mean distance O_{Br}^{2-}–B is about 4.44–4.96 Å and the O_{Br}–Br distance is 5.9 Å [9]. This is sufficiently large to prevent observation of superhyperfine interaction with neighbouring boron and bromine nuclear spin.

In figure 3, curves b–d display the behaviour of the EPR spectra of pure $Sr_2B_5O_9Br$ with temperatures below 120 K. A small deviation of the EPR line from O_{Br}^- centres at 336–337 mT can be explained by a change of the local symmetry of the defect with temperature. It is difficult to determine precise g-values of O_{Br}^- centres down to 8 K because of the appearance of the additional signal at about 340 mT. This signal must be due to another kind of defect, with very fast spin–lattice relaxation time above 120 K, since above this temperature it cannot be observed. The EPR signals at 340 mT and higher have g-values lower than g_e and originate from electron trapped centres [5]. Thus the EPR spectra shown in figure 3, curves b–d, represent the overlapped lines from electron and hole defects. In figure 3 the EPR spectra measured at 8 K one day and one week after irradiation, while keeping the sample at room temperature, are compared. The total intensity of the EPR signal decreases; however, the relative contribution from electron and hole trapped centres remains constant. This allows us to conclude that these electron/hole trapped centres are correlated, and at room temperature partly recombine with each other.

4.1.2. Optical absorption studies. The absorption energy of 365 nm seems to be too high for 1s → 2p transitions of F centres in bromides [10]. Instead this band can be attributed to the

absorption of O^-_{Br} centres. This assignment is based on three factors. First, the radiation induced EPR signal related to the O^-_{Br} centres was observed. Second, similar radiation absorption was observed in an oxygen contaminated BaF_2 crystal, and the absorption band of O^- centres was found in the UV region [11]. Finally, a very similar radiation induced absorption band at 360 nm was found in $Ba_5SiO_4Br_6:Eu^{2+}$ [12]. The only similar radiation induced defect is obvious in $Ba_5SiO_4Br_6$ and $Sr_2B_5O_9Br$ and is not an $F(Br^-)$ centre: it is an O^-_{Br}.

Radiation induced broad optical absorption bands have been observed in many oxide materials and this absorption was ascribed to holes trapped at O^{2-} centres. Attempts to explain the optical absorption of these $O^-(2p^5)$ centres as transitions between the p levels have met difficulties, since these transitions are forbidden and cannot cause the observed high oscillator strength of the absorption bands [13]. Another model was proposed in [14], where the optical absorption is explained by a hole transfer from one to another O^{2-} site near the defect. This model is more plausible, since the charge transfer process is known to exhibit a broad optical absorption band [15]. Thus the absorption band at 365 nm can be caused by a hole transitions from O^{2-}_{Br} to one of the 12 near oxygen atoms belonging to the borate network.

If an oxygen impurity is created in a bromine site during the synthesis, the anion vacancy is needed for charge compensation. After irradiation the anion vacancy can trap an electron and form an F centre. The radiation induced optical absorption band at 560 nm can be caused by the $1s \rightarrow 2p$ absorption band of $F(Br^-)$ centres. The position of the F-centre absorption band reflects the distance between the anion site and the surrounding first cation coordination sphere sites. The mean Sr–Br distance in bromoborates is 3.075 Å. For example, a Na–Br distance in NaBr is 3.0 Å, and the F-centre absorption band is located at 590 nm. Absorption energies of F centres in alkali bromides are about 2 eV (∼600 nm) [10]. Therefore, it is reasonable to assume that the broad absorption band at 560 nm in figure 4 is caused by $F(Br^-)$ centres.

Thus, the formation of $V_{Br} + O^{2-}_{Br}$ pairs during the synthesis in pure $Sr_2B_5O_9Br$ must be proposed. Created upon irradiation, $F(Br^-)$ and O^-_{Br} defects are stable at room temperature and give characteristic lines to EPR and optical absorption spectra.

The formation of the same types of defect can also be accepted in Ce^{3+} doped $Sr_2B_5O_9Br$. However, the optical absorption bands due to these defects are slightly shifted to a longer wavelength range (figure 5), which can be attributed to the presence of a high content of Ce^{3+} ions (1 mol%).

4.1.3. Origin of thermoluminescence in $Sr_2B_5O_9Br:Ce^{3+}$. Two TL peaks at 350 and 430 K were observed in $Sr_2B_5O_9Br:Ce^{3+}$ (figure 1). The high temperature peak is of interest from a practical point of view, because it is stable at room temperature and gives rise to intense TL and PSL. It is located at 430 K in Ce^{3+} doped bromoborates and at 415 K in Ce^{3+} doped chloroborates (figure 1). Hence, the high temperature TL peak can be somehow attributed to the defects related to the halide anion or its vacancy.

The formation of $V_{Br} + O^{2-}_{Br}$ pairs during the synthesis in pure $Sr_2B_5O_9Br$ was proposed above. Created upon irradiation, $F(Br^-)$ and O^-_{Br} defects are stable at room temperature. So, they are likely candidate defects for the TL peak at 430 K.

5. Conclusions

The EPR study on irradiated pure $Sr_2B_5O_9Br$ revealed a room temperature stable defect, which was attributed to the O^-_{Br} centre. The EPR signal from $F(Br^-)$ centres can be observed at temperatures below 120 K. The $1s \rightarrow 2p$ transitions of these $F(Br^-)$ centres cause an optical absorption band at 560 nm. The optical absorption band at 365 nm was attributed to O^- centres.

Thus electron and hole trapping in pure $Sr_2B_5O_9Br$ occurs in V_{Br} and O_{Br}^{2-} aggregates, which are created during the synthesis.

The EPR and radiation induced absorption measurements on Ce^{3+} doped $Sr_2B_5O_9Br$ revealed the same defects as in pure material. It is very likely that the same defects take part in the processes of thermally and photo-stimulated luminescence.

References

[1] Knitel M J, Bom V R, Dorenbos P, van Eijk C W E, Berezovskaya I V and Dotsenko V P 2000 *Nucl. Instrum. Methods* A **449** 578

[2] Sidorenko A V, Bos A J J, Dorenbos P, Le Masson N J M, Rodnyi P A, van Eijk C W E, Berezovskaya I V and Dotsenko V P 2002 *Nucl. Instrum. Methods* A **486** 160

[3] Schweizer S 2001 *Phys. Status Solidi* a **187** 335

[4] Sidorenko A V, Bos A J J, Dorenbos P, Rodnyi P A, van Eijk C W E, Berezovskaya I V and Dotsenko V P 2003 *J. Phys.: Condens. Matter* **15** 3471

[5] Marfunin A S 1979 *Spectroscopy, Luminescence and Radiation Centers in Minerals* (Berlin: Springer) chapter 7

[6] Dotsenko V P, Berezovskaya I V, Efryushina N P, Voloshinovskii A S, Dorenbos P and van Eijk C W E 2001 *J. Lumin.* **93** 137

[7] Griscom D L 1974 *J. Non-Cryst. Solids* **13** 251

[8] Hayes W (ed) 1974 *Crystal with the Fluorite Structure* (Oxford: Clarendon)

[9] Machida K, Ishino T, Adachi G and Shiokawa J 1979 *Mater. Res. Bull.* **14** 1529

[10] Agullo-Lopez F, Catlow C R A and Townsend P D 1988 *Point Defects in Materials* (New York: Academic)

[11] Eachus R S, McDugle W G, Nuttall R H D, Olm M T, Koschnick F K, Hangleiter Th and Spaeth J-M 1991 *J. Phys.: Condens. Matter* **3** 9327

[12] Schipper W J 1993 Luminescence and storage mechanism of new x-ray storage phosphors *PhD Thesis* Utrecht University, chapter 6

[13] Tohver H T, Henderson B, Chen Y and Abraham M M 1972 *Phys. Rev.* B **5** 3276

[14] Schirmer O F 1971 *J. Phys. Chem. Solids* **32** 499

[15] Dorenbos P 2003 *J. Phys.: Condens. Matter* **15** 8417